MiR-505-3p is a Repressor of the Puberty Onset in Female Mice

miR-505-3p and the puberty onset

Yuxun Zhou, Li Tong, Maochun Wang, Xueying Chang, Sijia Wang, Kai Li and Junhua Xiao*

The College of Chemistry, Chemical Engineering & Biotechnology, Donghua University, 2999 North Renmin Road, Songjiang, 200237 Shanghai, China

*Corresponding author: Junhua Xiao

Address: The College of Chemistry, Chemical Engineering & Biotechnology, Donghua University, 2999 North Renmin Road, Songjiang, 200237 Shanghai, China

Telephone number: +86-21-6779-2739

*To whom correspondence may be addressed. Email address: xiaojunhua@dhu.edu.cn （JX）

Data Availability Statement: All relevant data are within the paper and its supporting information files.

Competing interests: The authors have declared that no competing interests exist.

Abstract

Puberty onset is a complex trait regulated by multiple genetic and environmental factors. In this study, we narrowed a puberty related QTL down to a 1.7 Mb region on chromosome X in female mice and inferred miR-505-3p as the functional gene.

We conducted ectopic expression of miR-505-3p in the hypothalamus of prepubertal female mice through lentivirus-mediated orthotopic injection. The impact of miR-505-3p on female puberty was evaluated by the measurement of pubertal events and histological analysis. The results showed that female mice with overexpression of miR-505-3p in the hypothalamus manifested later puberty onset timing both in vaginal opening and ovary maturation, followed by weaker fertility lying in the longer interval time between mating and delivery, higher abortion rate and smaller litter size. We also constructed miR-505-3p knockout mice by CRISPR/Cas9 technology. MiR-505-3p knockout female mice showed earlier vaginal opening timing, higher serum gonadotrophin and higher expression of puberty-related gene, as well as its target gene *Srsf1* in the hypothalamus than their wild type littermates.

Srsf1 was proved to be the target gene of miR-505-3p that played the major role in this process. The results of RIP-seq (RNA Immunoprecipitation-sequencing) showed that SF2, the protein product of *Srsf1* gene, mainly bound to ribosome protein (RP) mRNAs in GT1-7 cells. The collective evidence implied that miR-505-3p/SRSF1/RP could play a role in the sexual maturation regulation of mammals.

Author summary

The puberty onset in mammals is a vital biological process that signals the acquisition of reproductive capacity. The initiation of puberty is triggered by the activation of hypothalamic pulsatile GnRH surge. The dysregulation of pubertal development shows relevance to later health risks of type 2

diabetes, cardiovascular disease, breast cancer and other health disorders. Recent progress indicates that a lot of genes play a role in the excitatory or inhibitory regulation of GnRH release. However, the detailed pathway of pubertal timing remains unclear. Our previous studies isolated an X-linked QTL that was associated with the timing of puberty in mice. In this study, we proved that miR-505-3p was a female puberty onset regulator based on data from positional cloning, ectopic expression and knockout mouse models. We also assigned *Srsf1* as the functional target gene of miR-505-3p underlying this process. The results of RIP-seq showed that SF2, the protein of *Srsf1* gene, preferential bound to ribosome protein (RP) mRNAs in GT1-7 cells. We propose that miR-505-3p/SF2/RP could play a role in the sexual maturation regulation of mammals.

Introduction

Puberty onset is an essential and complicated physiology process that relies on the activation of hypothalamic-pituitary-gonadal axis(HPGA).The pulsatile secretion of GnRH hormones from the specialized neurons in the hypothalamus trigger gonadal hormones secreting cascade that results in the maturation of sexual behaviors and signal the transition from non-reproductive juvenile into a fertility competent adult [1, 2]. The dysregulation of pubertal development shows relevance to later health risks for type 2 diabetes, cardiovascular disease, breast cancer and other health disorders [3].

The genetic and environmental factors involved in the regulation of puberty timing have been well characterized. The mutations in Gpr54 (a G protein–coupled receptor) gene could cause autosomal recessive idiopathic hypogonadotropic hypogonadism (iHH) in human, and the puberty regulating function of GPR54 was also revealed in mice with complementary genetic approaches [4-6]，which suggested a crucial role of GPR54 and its ligand Kisspeptin in the regulation of puberty.

During the last decade，novel central neuroendocrine pathways in the control of puberty have been

67 revealed. In 2017, genome-wide association studies including genotype data of up to ~370,000 women
68 identified 389 independent signals for age at menarche, ~250 genes were implicated via coding
69 variation or associated expression[7].The maternal imprinted gene MKRN3 was the first gene
70 identified with an inhibitory effect on GnRH secretion. It was related with central precocious puberty
71 by whole-exome sequencing of pedigree samples [8]. System biology strategies revealed that at least
72 three gene networks might contribute to the puberty onset [9].

73 In our previous studies, we isolated a QTL (quantitative trait locus) on Chromosome X affecting
74 the vaginal opening in female mice [10]. In this study, We narrowed the QTL down to a 1.7Mb region
75 by constructing 8 interval-specific congenic strains (ISCSs) between C57/BL6 (B6) and C3H/He(C3H)
76 mice. Among the genes in this region, miR-505-3p was assumed to be the potential candidate
77 according to the variation in its flanking sequence and gene expression levels between C3H and B6
78 mice, as well as its functional annotation. MicroRNAs are endogenous, small non-coding RNAs (~22nt
79 in length) silencing the gene expression at post-transcriptional level by targeting the 3' untranslated
80 region (UTRs) of mRNAs. MicroRNAs get involved in various biological processes [11]. Recent
81 evidence suggested that microRNAs also participated in the precise regulation of puberty onset [12].
82 MiR-505-3p usually serves as a biomarker of various diseases including primary biliary cirrhosis,
83 Parkinson's disease and inflammatory bowel disease [13-15]. Zucchi et al detected the downregulation
84 of miR-505-3p in newborn rat brain in response to the prenatal stress [16]. Moreover，miR-505-3p
85 was proved to induce apoptosis in MCF7-ADR cells, and functioned as a tumor suppressive miRNA
86 [17], its first validated target by experiments was the alternative splicing factor/splicing factor2
87 (ASF/SF2 or SRSF1) [18], which is a regulator of mTOR (the mammalian Target of Rapamycin)
88 pathway [19], while the activated mTOR signaling could accelerate the vaginal opening in female rats

89 [20]. Such indirect evidence tempted us to clarify the authentic relationship between miR-505-3p and
90 the mammalian puberty onset regulation.

91 In this study, we conducted overexpression of miR-505-3p in the hypothalamus of prepubertal
92 female mice through lentivirus-mediated orthotopic injection. We also constructed miR-505-3p
93 knockout mice (miR-505-3p -/-) by CRISPR/Cas9 technology. The impact of miR-505-3p on the
94 female puberty was evaluated by the measurement of pubertal events and histological analysis in these
95 genetically modified mice. The results showed that female mice with ectopic expression of miR-505-3p
96 in the hypothalamus manifested later puberty onset timing, compromised fertility, higher abortion rate
97 and smaller litter size. While miR-505 knockout female mice showed lightly earlier vaginal opening
98 and shorter interval time between mating and delivery. *Srsf1* was proved to be the target gene of
99 miR-505-3p that played the major role in this process. The results of RNA
100 Immunoprecipitation-Sequencing (RIP-Seq) showed SF2, the protein of *Srsf1* gene, mainly bound
101 ribosome protein (RP) mRNAs in GT1-7 cells.

102 All these results suggest that miR-505-3p may regulate the puberty onset via modulating the
103 expression of *Srsf1* gene and RP. They give us insights into a new regulating pathway involving
104 microRNA, SF2 and ribosome proteins in mammalian puberty onset.

105 **Results**

106 **MiR-505-3p was identified as a functional candidate gene in the QTL on chromosome X**

107 We have identified a 9.5Mb (2.5cM) QTL that regulates the puberty onset of female mice on
108 chromosome X in our previous work. To narrow down the QTL further, 8 interval-specific congenic
109 strains (ISCSs) with intervals within this region of B6 chromosome X were substituted into C3H
110 background in the N7 generation, in which we recorded the age at VO and body weights of all female

111 mice. Nonparametric tests showed that strain# 1~3, 7 and 8 showed significantly different VO age from
112 the parental strain C3H, while strain #4~6 didn't. Based on the QTL information and allele distribution
113 among those strains, we ascertained a shrunk QTL of about 1.6Mb between rs13483770 and
114 rs299055848 (Fig 1A, S1 Table).

115 There are 19 genes in the QTL region (rs13483770~rs299055848) on chromosome X, including
116 seven pseudogenes, four ncRNAs, seven protein-coding genes, and one microRNA gene. To screen for
117 the candidate gene(s), we referred to Sanger database to search for the DNA sequence variations
118 between C3H and B6 mice in this region. Data showed that there were no SNPs, short indels or
119 structural variants lying in the coding region, 5' or 3' UTR of these genes except for mir-505, as
120 sensible variations of 5 consecutive SNPs existed near 5' upstream region of mir-505 gene (S2 Table).
121 To confirm the results from Sanger database, we did DNA sequencing for the interested regions of the
122 19 genes, and found no exceptions. We compared the mRNA expression levels of the seven
123 protein-coding genes in HPG axis between B6 and C3H female mice in order to find out the
124 differentially expressed genes. Six of them were expressed in mouse HPGA except for the gene of
125 Gm7073, but they made hardly significant differences in the amount of accumulation between the two
126 strains, especially at the hypothalamus or pituitary (Fig 1B). On the other hand, miR-505-3p of B6 was
127 expressed higher in the hypothalamus than that of C3H (Fig 1C) at postnatal 15 days, and lower in the
128 pituitary and ovary at postnatal 45 days. We investigated the temporal and spatial expression pattern of
129 miR-505-3p in B6 female mice, and found that mir-505-3p was most abundant at hypothalamus in the
130 four tested tissues including pituitary, ovary and muscles (Fig1D); it reached its peak value of
131 expression at neonatal period (PD5) and decreased gradually afterwards (Fig1E), which implied its
132 inhibiting role in the sexual maturation process. The integrated evidence suggested that miR-505-3p

deserved further investigation as a functional candidate gene.

We constructed a GT1-7 cell line with stable overexpression of miR-505-3p named pGT1-7. In pGT1-7 cells, the expression level of miR-505-3p increased by 1500 times than the GT1-7 cells(S1 Fig) . We compared the expression profiling between pGT1-7 and negative control group GT1-7 (transfected with pLenti6.3-nc lentivirus) on DNA microarray, and found that some important puberty related genes, including *Kiss1* and *GnRH*, decreased in pGT1-7 cells. These results were confirmed by qRT-PCR assay (Fig1F), implying that miR-505-3p may participated in the puberty onset regulation through the inhibition of puberty related genes.

Ectopic expression of miR-505-3p in the hypothalamus influences the puberty onset timing and fertility of female mice

In order to investigate the influence of miR-505-3p on the puberty timing in female mice, we made miR-505-3p overexpressed in the hypothalamus of C57BL/6 (B6) female mice at postnatal 15 days by lentivirus-mediated orthotopic injection. In the window of post injection 5 to 40 days, the hypothalamic miR-505-3p overexpression maintained at a high level, reaching the peak at 10 days after injection (miR-505-3p-LV-treated=24.89±3.319, saline-treated=1.016±0.08129, untreated=1.096±0.2130, $P<0.0001$) . (S2 Fig)

After injection, the mice were weighted once every other day, and the miR-505-3p-LV-treated (abbreviated as LV-treated) female mice showed significant growth retardation compared with the untreated ones (Figure 2A). The vaginal opening in untreated mice were 2 days earlier than the LV-treated ones ($P<0.01$) (Figure2B).

After sexual maturation, the female mice were mated with wild-type experienced male mice to evaluate the long-term impact of hypothalamic miR-505-3p overexpression on reproduction. The LV-treated

155 female mice needed more time to procreate and had smaller newborn litters compared with the control
156 ones, the death rate of offspring before weaning increased in LV-treated mice as well (Figure2C and
157 2D). The Hematoxylin-eosin (HE) stained ovarian sections at various time showed the delay of the
158 formation of the preovulatory follicles and corpora luteas (CLs) in LV-treated female mice compared
159 with untreated ones, which provided explanation for the later birth of newborn offspring in LV-treated
160 mice, and the reduced number of newborn offsprings could be attributed to the deficiency or reduced
161 number of preovulatory follicles (Figure 3).
162 We found higher death rate of litters in LV-treated groups, and the rate of abortion in LV-treated
163 groups was 2.5 -fold higher than the two control groups. About 8 percent of LV-treated mice were
164 sterile in contrast with the control groups, in which no sterile mice were found (Figure 4A). The FISH
165 (florescence in situ hybridization) results of the brain section showed that the sterile female mouse had
166 stronger fluorescence signals near the third ventricle than the signals of its counterparts which had four
167 or eight litters, respectively. This finding suggested the level and the location of miR-505-3p
168 overexpression in the hypothalamus may influence the fertility phenotype of female mice(Figure 4B）.
169 **MiR-505-3p knockout mice showed an advanced onset of puberty and abnormal reproductive**
170 **phenotypes**
171 With the help of CRISPR/Cas9 technology, we obtained 41 living offsprings, and 16 of them carried
172 mutations in mir-505 cDNA region on their genome detected by DNA sequencing. Two pups with the
173 largest deletion (-17bp and -23bp, respectively) adjacent to the 5' end of miR-505 (S3 Fig) and in the
174 coding region of mature miR-505-5p were kept as founders to generate DKO miR-505-3p -/-), SKO
175 miR-505-3p +/-) and wild type mice for puberty onset trait investigation by backcrossing to B6 mice.
176 In DKO mice, the expressing level of miR-505-3p could hardly be tested, while in SKO mice, the

177 expressing level of miR-505-3p decreased by approximate half (S4 Fig). In female knockout mice, we
178 observed an increased growth rate and a larger body weight than wild type mice (Fig 5A), 3.57d and
179 3.87d advance in vaginal opening in SKO and DKO mice (Fig 5B), respectively. At PND45, the mass
180 of reproductive system was larger in knockout mice, indicating advanced sexual development in
181 knockout mice (Fig 5C).

182 We then analyzed serum levels of the pituitary gonadotropins luteinizing hormone (LH) and
183 follicle-stimulating hormone (FSH), and the results showed a remarkable increase in female knockout
184 mice (Fig 5D). Moreover, the size of the litter was larger in knockout mice than wild type, and
185 heterozygous knockout mice showed more dystocia in female mice and more dead off springs at 48h
186 (Table 1). Hematoxylin-eosin stained ovarian sections of miR-505-3p knockout mice showed more
187 corpus luteum (Fig 5E). *Srsf1*, *Kiss1* and *Gnrh* in hypothalamus of miR-505-3p knockout mice and
188 wild mice at different postnatal days were also detected, and the results showed knockout mice had
189 higher expression levels (Fig. 6).

190 **_Srsf1_ was proved to be a target gene of miR-505-3p in GT1-7 cell line**

191 We performed the Gene ontology analysis on the gene expression profilings data from the
192 microarray detection between pGT1-7 and GT1-7 cells. 1490 genes were upregulated and 604 genes
193 were downregulated in the pGT1-7 cells. Among these genes, we screened for the miR-505-3p target
194 genes on the TargetScan website. Four predicted genes, including *CD97*,*Hmbg1*,*Cadm1* and *Srsf1* with
195 high expression level in GT1-7 cells were assumed as the candidate target of miR-505-3p. Dual
196 luciferase reporter assay in HEK293 cells were performed to test the inhibitory effect of miR-505-3p
197 by binding to their 3'UTR. The results indicated that the other three genes except for CADM1 could be
198 the target genes of miR-505-3p (S5 Fig A, B). Integrated with their functional annotation, *Srsf1* was

199 selected preferentially for further investigation. Given that SF2 was proved to be a regulator of mTOR
200 signaling, we analyzed the phosphorylated status of S6K in pGT1-7 cells, but the amount of p-S6K
201 made no difference between GT1-7 and pGT1-7 cells (S5 Fig C).
202 The accumulation of SF2 protein was less in pGT1-7 cells than in GT1-7 cells (Fig.7A). Knocking
203 down *Srsf1* expression in GT1-7 by shRNA inhibited the expression of *Kiss1* and *Gnrh* simultaneously.
204 When the expression of *Srsf1* was rescued in pGT1-7 cells with *Srsf1*steadily overexpressed, the
205 expression level of *Kiss1* and *Gnrh* increased (Fig.7B). These results indicated that miR-505-3p may
206 inhibit the expression of puberty-related genes through *Srsf1*.
207 Moreover, *Srsf1*, *Kiss1* and *GnRH* in hypothalamus of miR-505-3p knockout mice and wild mice at
208 different postnatal days were also detected, and the result showed knockout mice had higher expression
209 levels (Fig. 7C).
210 **RIP-seq results showed SF2 mainly bound to RP mRNAs in GT1-7 cell line**
211 RNA immunoprecipitation sequencing (RIP-seq) was used to identify RNAs which bound to SF2
212 in GT1-7 cell line. The SF2 protein and its bounding RNAs were pulled down by SF2 specific
213 antibody, and the RNA component was sequenced by next generation sequencing. We pulled down
214 IgG protein and its bounding RNAs as one control sample, and the RNA extracted from GT1-7 was
215 another control sample. The RNA-seq data of the SF2 pull down sample was compare to the two
216 control data separately, and the two comparing results were highly consistent, SF2 protein mainly
217 bound ribosome related mRNAs in the GT1-7 cell (Table 2).
218 We performed the KEGG analysis on the transcriptome data compared pGT1-7 with GT1-7 cell.
219 The result showed ribosome and ribosome biogenesis in eukaryotes pathway were both affected in
220 pGT1-7 cell line (Fig. 8).

Discussion

Genetic strategies, such as positional cloning and association study, can be powerful tools to reveal the functional genes underlying the complex traits [10, 21-23]. We took the advantage of mouse models to make interval-specific congenic strains (ISCS) between C3H/He and C57/BL6 mice to finemap the QTLs related to the puberty onset and then reveal the candidate gene according to the sequence variation, expression differentiation and functional connection. To our knowledge, miR-505-3p is the first microRNA which was found by positional cloning as a puberty regulator in female mice.

Considerable progress has been made to decipher the molecular foundation of the pubertal timing [24-26]. Especially some studies revealed the potential epigenetic regulatory role of miRNAs and lncRNAs in female puberty[27]. Okabe et al indicate that the knockout of miR-200b and miR-429 can induce reduced fertility in female mice[28].Zhu et al show the variation in Lin28/let7 pathway can change the body size and onset of puberty in mice[29]. Furthermore, miR-132, miR--9 and miR-145 are also involved in the pubertal timing owing to their potential regulatory role of c-myc and Lin28[30,31]. In 2016, Messina et al. reported a microRNA switch that controled the rise of hypothalamus GnRH production before puberty in mice [32]. They provided direct evidence that the increasing expression of miR-200/429 and miR-155 in GnRH neurons during the infantile period lifted the repressive control of GnRH expression, by repressing ZEB1 and CEBPB, respectively [32]. These results suggested the existence of a multilayered and interconnected array of miRNAs and their target genes that control the puberty timing. Our results shows the overexpression of miR-505-3p in the hypothalamus can cause the delay of puberty timing and reduced fertility in female mice, and the results from miR-505-3p knockout mice supported the deduction, which could be a new member of this

243 regulating array.

244 We constructed a miR-505-3p ectopic expression female mouse model by lentiviral delivery.
245 Lentiviral vector as a versatile tool has been accessible to transfect post-mitotic neurons and induces
246 substantial, long-term transgene expression[33-35]. In our experiment, the miR-505-3p overexpression in
247 the mouse hypothalamus directed by lentivirus reached the peak (about 25 times as the control) on the
248 tenth day after injection and continued for at least 40 days (though declined to 8 times of the control),
249 which provided an ideal window to investigate the puberty onset and reproductive actions of the female
250 mice affected by the microRNA. Besides reverse transcription and real-time PCR，we performed in situ
251 hybridization for miR-505 detection using improved LNA-probes with high specificity and sensitivity.
252 The expression pattern of hypothalamic miR-505-3p detected by in situ hybridization can be used to
253 further elucidate the relationship between miR-505-3p function and the location of miR-505-3p in the
254 hypothalamus. Actually we have observed some connections between the injecting site and the
255 phenotypic distinction.

256 Finding out the target gene of miR-505-3p underlying the puberty onset in female mice can help
257 to tell the regulation mechanism of this complex trait. In our previous work, we identified one of the
258 important functions of miR-505-3p as that it was a crucial regulator for axonal elongation and
259 branching through modulating autophagy in neurons [36]. Atg12 was testified to be the key target gene
260 of miR-505-3p in this process, as its protein product ATG12 (autophagy-related 12) was an essential
261 component of the autophagy machinery during the initiation and expansion steps of autophagosome
262 formation. However, we did not find the influence of miR-505-3p overexpression on the amount of
263 ATG12 in GT1-7 cells, either in the mRNA expression profiling data or qRT-PCR detection, which
264 could be due to the different cell types we used. Autophagy is more active in neurons than in cultured

265 cells [37, 38], and the autophagy-related proteins in neurons could be not as sensitive to the microRNA
266 modulation as in the cultured GT1-7 cells. We found that when cultured in serum reduced medium, the
267 target gene of miR-505-3p became more sensitive to microRNA regulation in GT1-7 cells [39], which
268 implied that the decreased velocity of the protein synthesis under malnourished condition can help the
269 fine tuning of microRNAs on their targets. *Srsf1* is the first experimentally validated target gene of
270 miR-505-3p, and it was also a regulator of mTOR pathway, which was reported to participate in the
271 VO modulation in rats [20]. However, in miR-505-3p overexpressing pGT1-7 cells, the amount of the
272 marker of the activated mTOR signaling phosphorylated S6K was not affected, which implied that the
273 inhibition of the *Srsf1* expression by miR-505-3p did not influence the mTOR signaling in GT1-7 cells.
274 *Srsf1* is the archetype member of the SR (Serine an Argenine rich protein) family of splicing regulators
275 and has multiple functions in the cell nucleus and cytoplasm. Moreover, *Srsf1* is also a proto-oncogene
276 in cell malignant transformation [40, 41]. SF2 could bind to ribosomal proteins and help in mRNA
277 stability, transport, intracellular localization, and translation [42]. Ribosomal proteins play independent
278 key roles in the regulation of apoptosis, multidrug resistance and carcinogenesis [43,44], RPL22 can
279 inhibit Lin28B, RPS7 regulates PI3K/AKT and MAPK [45]. Our RIP results showed that SF2 bind to
280 the mRNA of ribosomal proteins preferentially which had not been reported before. The biological
281 significance of this selectivity has not been clarified though, it encourages us to assume that
282 miR-505-3p may affect the independent roles of ribosomal proteins by inhibiting SF2 in GT1-7 cells,
283 and the output of these series effects is the downregulation of puberty related genes. The potential
284 relationship between RP and the puberty development needs further elucidation. The function of
285 miR-505-3p as a puberty regulator in female mice has been revealed by cell and animal model, but the
286 underling mechanism still requires further researches.

Materials and methods:

Fine mapping of the puberty-related QTL on Chromosome X in mice

In our previous work, a significant puberty-related ChrX QTL of 2.5 cM was found by genome scanning, in a panel of 10 modified interval-specific congenic strains (mISCSs) in C57/BL6 and C3H/He mice [10]. In this study, the mice of the strain carrying the QTL were backcrossed with C3H mice. The resulting male F2 mice holding at least one recombination at the special interval were chosen and then backcrossed with female C3H to obtain N2 generation. The female N2 continued to mate with male C3H to generate N3 generation. N3 male mice holding only one recombination at the target interval were selected and continued to backcross with female C3H to generate N4. N4 mice siblings were crossed until N7 generation. At last, the age at VO of all female mice of N7 progenies was recorded. All modified ISCSs were verified by genotyping for the genetic markers on chromosome X. All animal procedures were approved by the Animal Ethics Committee of Donghua University, and all experiments were conducted in strict accordance with the National Institutes of Health Guide for the Use of Laboratory Animals.

DNA Extraction and Sequencing

DNA Extraction from the tail tip was performed using a DNA Extraction Kit (Tiangen, China), followed by the instructions provided by the manufacturer. All gene sequence data were from NCBI database. And the primers were designed by Primer3 (http://frodo.wi.mit.edu/primer3/) and synthesized by Shanghai Sangon Biotech Ltd. PCR was performed in 15 μL reaction mix containing 3 μL DNA template, 200 nM of each PCR primer, 0.25 mM of each dNTP, 3 nM MgCl2, 1.5 μL 10×PCR Buffer and 1 U Hot start DNA Polymerase (Tiangen, China) covered by mineral oil. The reaction was carried out at 95℃ for 15 min, followed by 95℃ 30 sec, 55℃ 0.5

309 min, 72℃ 1 min, 35 cycles. The purified PCR products were sequenced by 3730XL sequencing
310 instrument (ABI, USA).

311 **SNP database querying between C3 and B6 mice**

312 All SNPs between C3 and B6 mice in the QTL region (rs13483770~rs299055848) on chromosome X
313 were queried from Mouse Genome Project in Sanger Database
314 (http://www.sanger.ac.uk/science/data/mouse-genomes-project).

315 **qRT-PCR**

316 Total RNA from hypothalamus or 10^6 cells was isolated using Trizol reagent (Invitrogen, USA) in line
317 with the manufacturer's protocol. 1ug of total RNA was reverse-transcribed with oligo-dT (for mRNA
318 detection) or microRNA specific primer (for microRNA detection) by RevertAid First strand cDNA
319 synthesis Kit (ThermoFisher, USA). Real-time PCR was performed using SuperReal PreMix Plus
320 (TIANGEN,Beijing, China) on 7500 Real-time PCR System (Applied Biosystems) and normalized to
321 *Actb* (for mRNA) or miR-16 (for microRNA). All reactions were run in triplicate and included no
322 template control for each gene. All PCR primers were listed in S3 Table.

323 **Generation of hypothalamic miR-505 overexpressing mice**

324 C57/BL6 (B6) inbred mice were purchased from Shanghai SLAC Laboratory Animals Co.LTD
325 (Shanghai,China). The miR-505-3p carrying lentivirus delivery was performed on female mice at
326 postnatal 12-15d weighted at 5.2-5.6 g. After 1% sodium pentobarbital anaesthesia, mice were fixed on
327 stereotaxic apparatus (STOELTING, USA). According to Paxions et al[21] ,The hypothalamic
328 stereotaxic coordinates were carried out relative to the bregma (anteroposterior [AP]=-1.53mm and
329 lateral [L]=±0.24mm) and to the skull (dorsoventral[DV]=-5.3mm). The injection of lentiviral
330 preparation (2.83E+08 IU/ml, 900 nl per sample) was at the rate of 30 μL/min. Saline were also

injected to the female mice at the same condition to be used as controls. After injection, the mice were kept at 37°C till recovered from anesthesia. Afterwards, the mice were put back to their mothers for further investigation.

Cryostat section

Mice were under 1% sodium pentobarbital anesthesia and perfused by 0.9% saline. When the color of liver and lung become pale, saline was replaced by 4% paraformaldehyde to fix the tissues. Then the brains and ovaries were taken out and kept in paraformaldehyde solution at 4 ℃ overnight. The fixed brains and ovaries were dehydrated by glucose solution and cut into sections using Cryotome (Thermo,USA). The thickness of brain and ovary sections was 15μm and 20μm, respectively. The sections were attached to slides which were pretreated with potassium dichromate and embedded in polylysine. Slides were stored at -80 ℃ until objected to FISH and HE staining, respectively.

In situ hybridizations

Brain sections were taken out from -80 ℃ and dried at room temperature for at least 10 min. The sections were fixed by 4% paraformaldehyde and pretreated withj Triton x -100 and Proteinase K to improve the tissue permeability. After pre-hybridization, sections were hybridization with diluted digoxigenin (DIG)-labeled LNA probes for miR-505-3p, (5'-AGAAAACCAGCAAGTGTTGACG-3') at 55℃ overnight. Then the sections were washed and incubated with Horseradish Peroxidase（HRP) conjugated anti-DIG antibodies(Abcam,Shanghai,China） at 4.℃ overnight. The fluorescent signals were amplified using TSA™Cyanine 5 Systerm (PerkinElmer,USA) and detected by inverted phase contrast fluorescence microscope (Olympus, Japan).

Measurement of pubertal events and fertility analysis

The animals were housed under the specific pathogen free (SPF) standard conditions with a 12 h

353 light/dark cycle and adequate water and food. Injected female pups were caged with their mothers
354 again and weighed every two days. After weaned at postnatal 21d, the mice were examined daily for
355 the vaginal opening. They were mated with fertile male mice at the age of 8 weeks at the ratio of two to
356 one. Female mice with drastic body weight gaining were assumed to be pregnant and were separated
357 from male mice into a single cage. The interval time between mating and delivery was recorded.
358 Female mice that failed to be pregnant for more than one month were regarded as infertile. The rate of
359 infertility in female mice and the death rate of newborns were calculated. Mice with vacant virion or
360 saline injected were used as control.

361 **Hormone detection**

362 Serum LH and FSH were extracted by mouse orbital blood sampling. The detection of LH or FSH was
363 performed using Mouse LH ELISA KIT or Mouse FSH ELISA KIT(Elabscience,Wuhan,China)
364 according to manufacture's procedures, respectively. The standard curve was plotted by CurveExpert
365 1.4 software, which was also used to calculate the concentration of LH and FSH referring to the
366 standard curve.

367 **Histological analysis**

368 Ovarian sections were taken out from -80 ℃ and dried for at least 10 minutes. Then the sections were
369 dehydrated by ethanol and stained by hematoxylin and eosin (HE). The morphology of ovaries was
370 detected by light microscope (Olympus, Japan).

371 **Generation of miR-505 knockout mice**

372 The miR-505 knockout mice were generated in CRISPR/Cas9 technology by The Animal Facility of
373 Indtitute of Neuroscience, Chinese Academy of Sciences. Female B6 mice were superovulated using
374 pregnant mare serum gonadotropin (PMSG) and were injected with human chorionic gonadotropin

(HCG) after 48 h. The superovulated female mice were mated with B6 stud males, and fertilized eggs were collected from their oviducts after 36 hours. Two sgRNAs were designed to guide Cas9 targeting the pre-miR-505 locus (S1 Fig). A mixture of transcribed Cas9 mRNA and sgRNA was microinjected into zygotes of B6 mouse. The injected zygotes were transferred into the uterus of pseudopregnant female mice immediately after injection. The pregnant mice were housed in standard cages on a 12 h light/dark cycle with *ad libitum* access to food and water till delivery.

The pups were taken by tail clips and their DNAs were extracted for sequencing. Pups with large deletions in pre-mir-505 region were reserved as founders. The generated male and female founders were mated with wild-type B6 mice at the age of 40 days. The heterozygote F1 mice were self-crossed to generate double knockout (DKO), single knockout (SKO) and wild type mice for further puberty events study. The resulting female mice were genotyped by PCR detection with the primers, forward: 5'-AAACCAGCAAGTGTTGACGC, reverse: 5'-CCCTGTTTGTCACTTGCAGA, The lengths of the PCR products were 120bp for wild type, 103bp、120bp and 97bp、120bp for heterozygous, and 97bp and 103bp for homozygous knockout mice.

Construction of miR-505-3p stable over-expressed and *Srsf1* knockdown GT1-7 cell line

The double strand DNA sequence of miR-505-3p was cloned into the pLenti6.3/V5-DEST lentiviral expression vector (Invitrogen, USA). The target sequence of shRNA for *Srsf1* (5'-GCCCAGAAGTCCAAGTTAT-3') and non-specific shRNA (5'-TTCTCCGAACGTGTCACGT-3') were synthesized and cloned into the PLKD-CMV-R&PR-U6-shRNA lentiviral expression vector. The resulting lentivirus vectors were were packaged into virions by Obio Technology Co. LTD (Shanghai, China). The virions were used to infect GT1-7 cells. Cells were seeded 100000 cells per well in twenty-four-well plate and cultured in DMEM medium with 10% FBS (Gibco, USA). After 4 days of

transfection, cells were selected under antibiotics according to the vector's resistances for 14 days. After 10 days of expansion without antibiotics, the surviving cells were harvested for further investigation. GT1-7 cells with miR-505-3p overexpression were named as pGT1-7.

We used GeneChip Mouse Transcriptome Assay 1.0 (Affymetrix, USA) to get the transcriptome data of pGT1-7, and GT1-7 as the control. Differential expressed genes were used to perform KEGG analysis based on Kyoto Encyclopedia of Genes and Genomes database.

Cell culture and RIP-seq

GT1-7 cells are immortalized cell lines derived from mouse hypothalamic neurosecretory neurons which provide an ideal model system for study of that regulate reproduction as their similarity to GnRH neurons, such as the synthesis, processing, and pulsatile secretion of GnRH (gonadotropin-releasing hormone)[47]. GT1-7 cells applied in this study were kindly provided by Professor Xiaoying Li of Shanghai Clinical Center for Endocrine and Metabolic Diseases, Shanghai Jiaotong University suggested by Dr. Pamela Mellon at University of California, San Diego. We performed RNA immunological precipitation (RIP) assays followed by high-throughput sequencing in SF2 pulldown of GT1-7 cell, IgG pulldown and total RNA as the control. Briefly, after cell lysis, 10% of sample removed for input stored at -80℃ until ready to perform RNA purification. The input sample is used to calculate RIP yields, and may also be used to evaluate the quality of the RNA. Add RNA binding SF2 protein-specific antibody or negative control IgG to supernatant. Incubate with rotation at 4℃ for overnight. Add washed protein A+G Agarose to each IP sample and incubate with rotation at 4 ℃ for 2 hours, then wash off unbound material and remove supernatants. RNAs bound to RNA-binding protein were purified with Trizol and sequenced by NGS.

Acknowledgments

We appreciate Professor Xiaoying Li in Shanghai Clinical Center for Endocrine and Metabolic Diseases, Shanghai Jiaotong University for providing GT1-7 cells. We also thank Yu Li and Li Chen for help doing some experiments, Fuyi Xu for the assistance of data analysis, and Xiaoning Li for the assistance of manuscript writing.

References

1. Holder MK, Blaustein JD. Puberty and adolescence as a time of vulnerability to stressors that alter neurobehavioral processes. Front Neuroendocrinol. 2014;35(1):89-110. doi: 10.1016/j.yfrne.2013.10.004.

2. Sisk CL, Foster DL. The neural basis of puberty and adolescence. Nature Neuroscience. 2004;7:1040. doi: 10.1038/nn1326.

3. Day FR, Perry JR, Ong KK. Genetic Regulation of Puberty Timing in Humans. Neuroendocrinology. 2015;102(4):247-55. doi: 10.1159/000431023.

4. Kostrzewa E, Kas MJ. The use of mouse models to unravel genetic architecture of physical activity: a review. Genes Brain Behav. 2014;13(1):87-103. doi: 10.1111/gbb.12091.

5. Seminara SB, Messager S, Chatzidaki EE, Thresher RR, Acierno Jr JS, Shagoury JK, et al. The GPR54 gene as a regulator of puberty. New England Journal of Medicine. 2003;349(17):1614-27. doi: 10.1056/NEJMoa035322.

6. de Roux N, Genin E, Carel JC, Matsuda F, Chaussain JL, Milgrom E. Hypogonadotropic hypogonadism due to loss of function of the KiSS1-derived peptide receptor GPR54. Proc Natl Acad Sci U S A. 2003;100(19):10972-6. doi: 10.1073/pnas.1834399100.

7. Day FR, Thompson DJ, Helgason H, Chasman DI, Finucane H, Sulem P, et al. Genomic analyses identify hundreds of variants associated with age at menarche and support a role for puberty timing in

441 cancer risk. Nat Genet. 2017;49(6):834-41. doi: 10.1038/ng.3841.

442 8. Abreu AP, Dauber A, Macedo DB, Noel SD, Brito VN, Gill JC, et al. Central precocious puberty

443 caused by mutations in the imprinted gene MKRN3. N Engl J Med. 2013;368(26):2467-75. doi:

444 10.1056/NEJMoa1302160.

445 9. Lomniczi A, Wright H, Castellano JM, Sonmez K, Ojeda SR. A system biology approach to identify

446 regulatory pathways underlying the neuroendocrine control of female puberty in rats and nonhuman

447 primates. Horm Behav. 2013;64(2):175-86. doi: 10.1016/j.yhbeh.2012.09.013.

448 10. Zhu W, Fan Z, Zhang C, Guo Z, Zhao Y, Zhou Y, et al. A dominant X-linked QTL regulating

449 pubertal timing in mice found by whole genome scanning and modified interval-specific congenic

450 strain analysis. PLoS One. 2008;3(8):e3021. doi: 10.1371/journal.pone.0003021.

451 11. Bartel D P. MicroRNAs: genomics, biogenesis, mechanism, and function. Cell, 2004, 116(2):

452 281-297. doi: 10.1016/S0092-8674(04)00045-5

453 12. Lomniczi A, Wright H, Ojeda SR. Epigenetic regulation of female puberty. Front

454 Neuroendocrinol. 2015;36:90-107. doi: 10.1016/j.yfrne.2014.08.003.

455 13. Ninomiya M, Kondo Y, Funayama R, Nagashima T, Kogure T, Kakazu E, et al. Distinct

456 microRNAs expression profile in primary biliary cirrhosis and evaluation of miR 505-3p and

457 miR197-3p as novel biomarkers. PLoS One. 2013;8(6):e66086. doi: 10.1371/journal.pone.0066086.

458 14. Khoo SK, Petillo D, Kang UJ, Resau JH, Berryhill B, Linder J, et al. Plasma-based circulating

459 MicroRNA biomarkers for Parkinson's disease. J Parkinsons Dis. 2012;2(4):321-31. doi:

460 10.3233/JPD-012144.

461 15. Pekow JR, Kwon JH. MicroRNAs in Inflammatory Bowel Disease. Inflammatory Bowel Diseases.

462 2012;18(1):187-93. doi: 10.1002/ibd.21691.

463 16. Zucchi FC, Yao Y, Ward ID, Ilnytskyy Y, Olson DM, Benzies K, et al. Maternal stress induces
464 epigenetic signatures of psychiatric and neurological diseases in the offspring. PLoS One.
465 2013;8(2):e56967. doi: 10.1371/journal.pone.0056967.
466 17. Yamamoto Y, Yoshioka Y, Minoura K, et al. An integrative genomic analysis revealed the
467 relevance of microRNA and gene expression for drug-resistance in human breast cancer cells. Mol
468 Cancer. 2011 Nov 3; 10:135. doi: /10.1186/1476-4598-10-135
469 18. Verduci L, Simili M, Rizzo M, Mercatanti A, Evangelista M, Mariani L, et al. MicroRNA
470 (miRNA)-mediated interaction between leukemia/lymphoma-related factor (LRF) and alternative
471 splicing factor/splicing factor 2 (ASF/SF2) affects mouse embryonic fibroblast senescence and
472 apoptosis. J Biol Chem. 2010;285(50):39551-63. doi: 10.1074/jbc.M110.114736.
473 19. Karni R, Hippo Y, Lowe SW, Krainer AR. The splicing-factor oncoprotein SF2/ASF activates
474 mTORC1. Proc Natl Acad Sci U S A. 2008;105(40):15323-7. doi: 10.1073/pnas.0801376105.
475 20. Roa J, Garcia-Galiano D, Varela L, Sanchez-Garrido MA, Pineda R, Castellano JM, et al. The
476 mammalian target of rapamycin as novel central regulator of puberty onset via modulation of
477 hypothalamic Kiss1 system. Endocrinology. 2009;150(11):5016-26. doi: 10.1210/en.2009-0096.
478 21. He C, Kraft P, Chen C, Buring JE, Paré G, Hankinson SE, et al. Genome-wide association studies
479 identify loci associated with age at menarche and age at natural menopause. Nature Genetics.
480 2009;41:724. doi: 10.1038/ng.385.
481 22. Ong KK, Elks CE, Li S, Zhao JH, Luan Ja, Andersen LB, et al. Genetic variation in LIN28B is
482 associated with the timing of puberty. Nature Genetics. 2009;41:729. doi: 10.1038/ng.382.
483 23. Perry JRB, Stolk L, Franceschini N, Lunetta KL, Zhai G, McArdle PF, et al. Meta-analysis of
484 genome-wide association data identifies two loci influencing age at menarche. Nature Genetics.

485 2009;41:648. doi: 10.1038/ng.386.

486 24. Topaloglu AK, Reimann F, Guclu M, Yalin AS, Kotan LD, Porter KM, et al. TAC3 and TACR3

487 mutations in familial hypogonadotropic hypogonadism reveal a key role for Neurokinin B in the central

488 control of reproduction. Nature Genetics. 2008;41:354. doi: 10.1038/ng.306.

489 25. Uenoyama Y, Tsukamura H, Maeda K. KNDy neuron as a gatekeeper of puberty onset. J Obstet

490 Gynaecol Res. 2014;40(6):1518-26. doi: 10.1111/jog.12398.

491 26. Xu Y, Faulkner LD, Hill JW. Cross-Talk between Metabolism and Reproduction: The Role of

492 POMC and SF1 Neurons. Front Endocrinol (Lausanne). 2011;2:98. doi: 10.3389/fendo.2011.00098.

493 27. Avendaño MS, Vazquez MJ, Tena-Sempere M. Disentangling puberty: novel neuroendocrine

494 pathways and mechanisms for the control of mammalian puberty. Human Reproduction Update.

495 2017;23(6):737-63. doi: 10.1093/humupd/dmx025.

496 28. Hasuwa H, Ueda J, Ikawa M, et al. miR-200b and miR-429 function in mouse ovulation and are

497 essential for female fertility. Science, 2013, 341(6141): 71-73. doi: 10.1126/science.1237999.

498 29. Zhu H, Shah S, Shyh-Chang N, Shinoda G, Einhorn WS, Viswanathan SR, et al. Lin28a transgenic

499 mice manifest size and puberty phenotypes identified in human genetic association studies. Nature

500 Genetics. 2010;42:626. doi: 10.1038/ng.593.

501 30. Sangiao-Alvarellos S, Manfredi-Lozano M, Ruiz-Pino F, Navarro VM, Sanchez-Garrido MA, Leon

502 S, et al. Changes in hypothalamic expression of the Lin28/let-7 system and related microRNAs during

503 postnatal maturation and after experimental manipulations of puberty. Endocrinology.

504 2013;154(2):942-55. doi: 10.1210/en.2012-2006.

505 31. Sachdeva M, Mo Y-Y. miR-145-mediated suppression of cell growth, invasion and metastasis.

506 American Journal of Translational Research. 2010;2(2):170-80.

507 32. Messina A, Langlet F, Chachlaki K, Roa J, Rasika S, Jouy N, et al. A microRNA switch regulates
508 the rise in hypothalamic GnRH production before puberty. Nat Neurosci. 2016;19(6):835-44. doi:
509 10.1038/nn.4298.
510 33. Eleftheriadou I, Mazarakis N D. Lentiviral Vectors for Gene Delivery to the Nervous System. Gene
511 Delivery and Therapy for Neurological Disorders, 2015,pp 23-66.
512 34. Zhao W, Dong Y, Wu C, Ma Y, Jin Y, Ji Y. MiR-21 overexpression improves osteoporosis by
513 targeting RECK. Mol Cell Biochem. 2015;405(1-2):125-33. doi: 10.1007/s11010-015-2404-4.
514 35. Zeng L, He X, Wang Y, Tang Y, Zheng C, Cai H, et al. MicroRNA-210 overexpression induces
515 angiogenesis and neurogenesis in the normal adult mouse brain. Gene Therapy. 2013;21:37. doi:
516 10.1038/gt.2013.55.
517 36. Yang K, Yu B, Cheng C, Cheng T, Yuan B, Li K, et al. Mir505–3p regulates axonal development
518 via inhibiting the autophagy pathway by targeting Atg12. Autophagy. 2017;13(10):1679-96. doi:
519 10.1080/15548627.2017.1353841.
520 37. Mizushima N, Yoshimori T, Levine B. Methods in mammalian autophagy research. Cell.
521 2010;140(3):313-26. doi: 10.1016/j.cell.2010.01.028.
522 38. Kovács AL, Telbisz Á, Eldib A. Autophagy in hepatocytes and erythropoietic cells isolated from
523 the twenty-one day old rat embryo. Acta Biologica Hungarica. 2001;52(4):417-33. doi:
524 10.1556/ABiol.52.2001.4.7.
525 39. Yang K, Tong L, Li K, Zhou Y, Xiao J. A SRSF1 self-binding mechanism restrains Mir505-3p
526 from inhibiting proliferation of neural tumor cell lines. Anti-Cancer Drugs. 2018;29(1):40-9. doi:
527 10.1097/cad.0000000000000564.
528 40. Karni R, de Stanchina E, Lowe SW, Sinha R, Mu D, Krainer AR. The gene encoding the splicing

529 factor SF2/ASF is a proto-oncogene. Nature Structural &Amp; Molecular Biology. 2007;14:185. doi:
530 10.1038/nsmb1209.
531 41. Ghigna C, Giordano S, Shen H, Benvenuto F, Castiglioni F, Comoglio PM, et al. Cell motility is
532 controlled by SF2/ASF through alternative splicing of the Ron protooncogene. Mol Cell.
533 2005;20(6):881-90. doi: 10.1016/j.molcel.2005.10.026.
534 42. Shao R, Wang X, Weijdegard B, Norstrom A, Fernandez-Rodriguez J, Brannstrom M, et al.
535 Coordinate regulation of heterogeneous nuclear ribonucleoprotein dynamics by steroid hormones in the
536 human fallopian tube and endometrium in vivo and in vitro. Am J Physiol Endocrinol Metab.
537 2012;302(10):E1269-82. doi: 10.1152/ajpendo.00673.2011.
538 43. Song MJ, Jung CK, Park CH, Hur W, Choi JE, Bae SH, et al. RPL36 as a prognostic marker in
539 hepatocellular carcinoma. Pathol Int. 2011;61(11):638-44. doi: 10.1111/j.1440-1827.2011.02716.x.
540 44. Provost E, Bailey JM, Aldrugh S, Liu S, Iacobuzio-Donahue C, Leach SD. The tumor suppressor
541 rpl36 restrains KRAS(G12V)-induced pancreatic cancer. Zebrafish. 2014;11(6):551-9. doi:
542 10.1089/zeb.2014.1024.
543 45. Zhou X, Liao WJ, Liao JM, Liao P, Lu H. Ribosomal proteins: functions beyond the ribosome. J
544 Mol Cell Biol. 2015;7(2):92-104. doi: 10.1093/jmcb/mjv014.
545 46. Paxinos G, Franklin K B J. The mouse brain in stereotaxic coordinates. Gulf Professional
546 Publishing, 2004.
547 47. Mellon PL, Windle JJ, Goldsmith PC, Padula CA, Roberts JL, Weiner RI. Immortalization of
548 hypothalamic GnRH by genetically targeted tumorigenesis. Neuron. 1990;5(1):1-10. doi:
549 10.1016/0896-6273(90)90028-E

550 Figure Legends

551 **Fig 1**. The evidence of miR-505-3p being a candidate gene in the puberty onset related QTL on
552 chromosome X. A: schematic representation of the ISCSs and control strains. The genotype on
553 chromosome X for each of the 8 congenic strains is represented by the horizontal bars. Green portions
554 indicate a known homozygous B6 segment, blank portions represent a known homozygous C3
555 segment, and hatched regions depict an area where a crossover between C3 and B6 occurred. The
556 dotted lines indicate the boundary of the refined QTL. B: The expression situation of six protein-coding
557 genes in the QTL in HPG axis in B6 and C3 strains. H: hypothalamus; P: pituitary; O:overy. C: The
558 expression difference of miR-505-3p in HPG axis between B6 and C3H mice. D: The Spatial-specific
559 expression of miR-505-3p in different time point of B6 mice. E: The temporal-specific expression of
560 miR-505-3p in different tissues of B6 mice. F: The expression level of puberty related genes in GT1-7
561 and pGT1-7cells. Bars are means and vertical bars represent SEM (* P<0.05, ** P<0.01, *** P<0.001).
562 **Fig 2.** The influence of miR-505-3p ectopic expression in the hypothalamus on the body weight, VO
563 timing and fertility of the tested mice. A: the growth curve of the mice B: the VO time of the tested
564 mice; C: The interval time between mating with male mice and delivery （LV-treated=25.83 ±1.144d，
565 saline-treated=24.33 ±1.247d，untreated=22.92 ±0.8307，P<0.05,*）; D: the death rate of offspring
566 before weaning of the tested mice （newborn offspring：LV-treated=6.100 ±0.7944,
567 saline-treated=7.111 ±0.3093, untreated=7.949 ±0.1798, ; dead offspring：LV-treated=2.1110±0.6256,
568 saline-treated=0.1111 ±0.1111，untreated=0.2564 ±0.1085. P<0.05 *, P<0.01**)
569 **Fig 3**. The HE stained ovarian sections at various time
570 **Fig 4.** Fertility analysis and in situ hybridization of the brain section. A: Pie chart shows the percentage
571 of female mice which had different number of dead litters and the rate of abortion and infertility among
572 the three groups; B: Images of coronal sections showed the fluorescence signals of hypothalamic

573 miR-505-3p detected by in situ hybridization among one sterile, one reduced fertility, one normal,
574 saline-treated and untreated mice using U6 、miR-505-3p and scrambled LNA probes ,respectively.

575 **Fig 5**: **The phenotype of miR-505-3p knockout mice.** A: The growth curve of the DKO, SKO and
576 WT mice; B: the percentage of female mice attaining VO at different time point; C: the mass of
577 reproductive system at PND45; D: The serum LH and FSH of the DKO and WT mice; E: HE stained
578 ovarian sections of the tested mice. (*：P<0.05, **：P<0.01)

579 **Fig 6**. The **expression level of Srsf1, Kiss1 and GnRH in the hypothalamus of mice at PND15,**
580 **PND25, PND45.**

581 **Fig 7: miR-505-3p and its target gene *Srsf1* play a role in the puberty onset regulation.** A: The
582 translation of Srsf1 was inhibited by miR-505-3p in pGT1-7 cell line. B: The expression level of
583 puberty related genes in pGT1-7 after Srsf1 overexpression. Bars are means and vertical bars represent
584 SEM (* P<0.05, ** P<0.01, *** P<0.001, ns no statistical significance). C: Srsf1, Kiss1 and GnRH
585 expression level in the hypothalamus of miR-505-3p KO mice at PND15, PND25, PND45

586 **Fig 8. Pathway analysis of differentially expressed genes between GT1-7 and pGT1-7 cell.**

587

588 **Table 1.** Effect of miR-505-3p deficiency on female fertility.

Strains	Litters	Dystocia in female (%)	Mean litter size	*P* [b]	Dead offspring (% at 48h)
WT	30	0	6.032 (0.3485)		1.07
miR-505-3p +/-	35	31.4	7.125 (0.3677)	0.0373	29.8

589 Note：a: Values are the mean (s.e.m.). b: P value for mean litter size compared to wild type.

590

591 **Table 2. Top 10 gene list of SF2 pull down sample RNA-seq data compare to two control**

592 **samples' data separately**

gene	sample_1	sample_2	value_2	log2(fold_change)	gene	sample_1	sample_2	value_2	log2(fold_change)
Eif4a2	IgG	SRSF1	1514 3.60	4.9594	**Rpl19**	total RNA	SRSF1	1474 1.80	5.1391
Rpl19	IgG	SRSF1	854.94	5.6497	**Rpl7**	total RNA	SRSF1	6198.61	4.5250
Ppm1h	IgG	SRSF1	580.72	2.9438	**Rps9**	total RNA	SRSF1	8300.55	4.0617
Rpl21	IgG	SRSF1	571.01	4.7366	**Rpl21**	total RNA	SRSF1	6480.69	3.6071
Rps14	IgG	SRSF1	512.69	4.3983	**Rps14**	total RNA	SRSF1	7648.64	3.0312
Psmd4	IgG	SRSF1	440.08	3.4028	Ccdc124	total RNA	SRSF1	2878.78	5.8550
Rps9	IgG	SRSF1	384.78	3.8331	Dus1l	total RNA	SRSF1	1316.45	5.1459
Nudc	IgG	SRSF1	334.29	5.0492	Psmc4	total RNA	SRSF1	3105.27	4.8709
Rpl7	IgG	SRSF1	332.53	4.0535	Nudc	total RNA	SRSF1	5493.75	4.8040

Rund		SRSF	317.4		Tim	total	SRSF	1080.	
	IgG			3.7359					4.7274
c3a		2	4		m23	RNA	2	61	

593

594

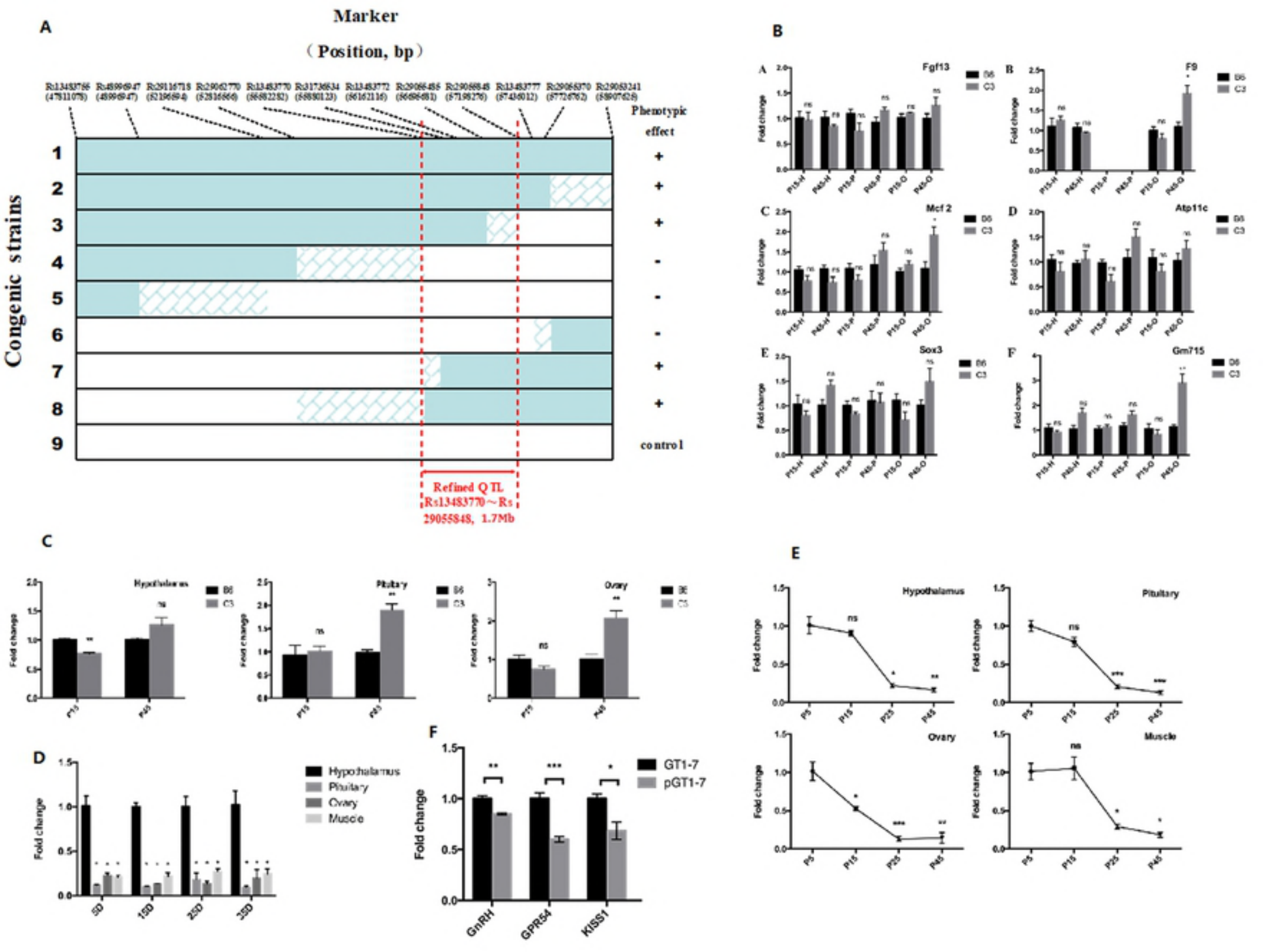
A
Marker
（Position, bp）
Congenic strains
Phenotypic effect
control
Refined QTL
Rs13483770～Rs
29055848, 1.7Mb
B
Fgf13
F9
Mcf2
Atp11c
Sox3
Gm715
B6
C3
Fold change
C
Hypothalamus
Pituitary
Ovary
D
Hypothalamus
Pituitary
Ovary
Muscle
5D
15D
25D
35D
E
Hypothalamus
Pituitary
Ovary
Muscle
P5
P15
P25
P45
F
GT1-7
pGT1-7
GnRH
GPR54
KISS1

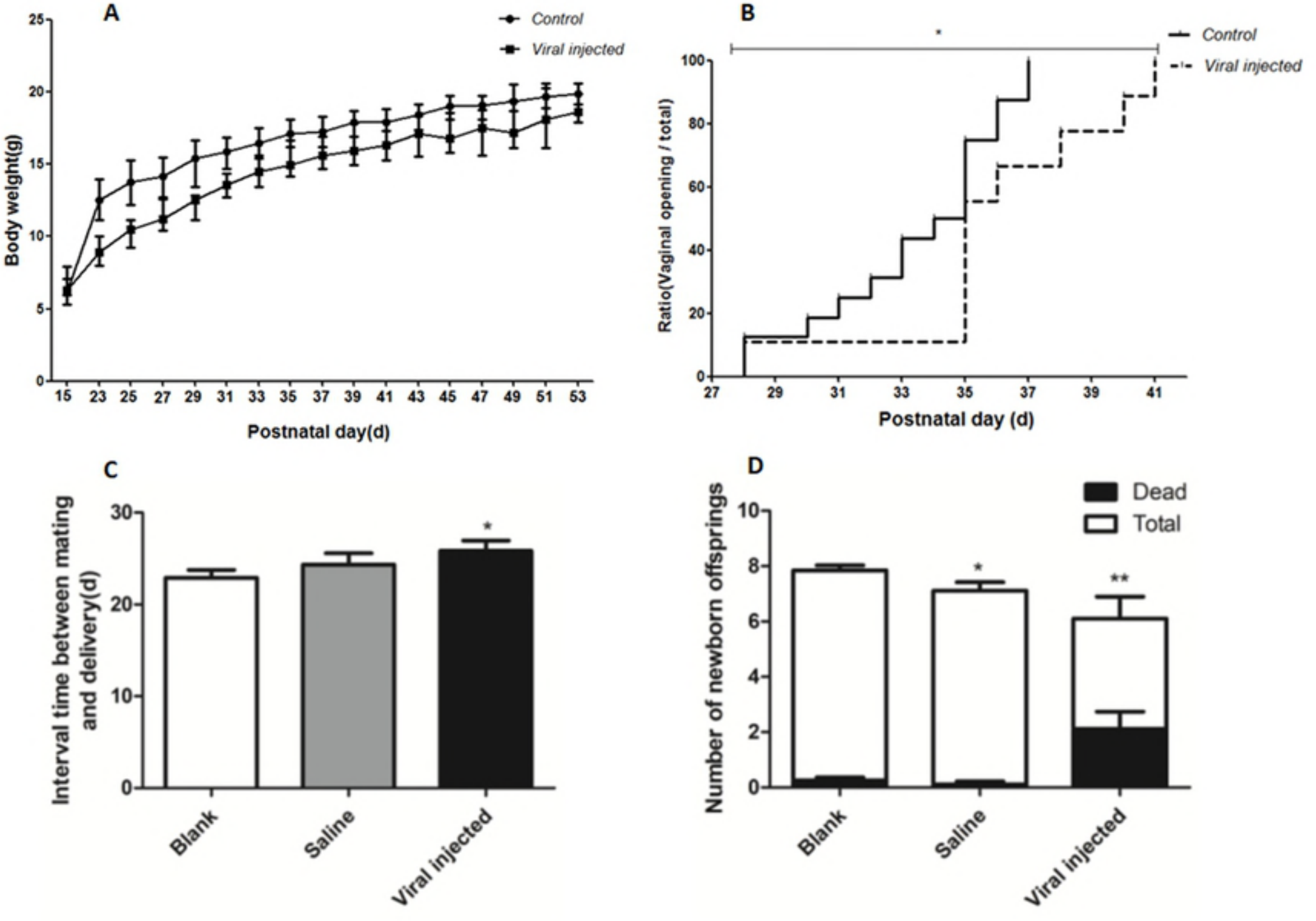
A
Control
Viral injected
Body weight(g)
Postnatal day(d)
B
Control
Viral injected
Ratio(Vaginal opening / total)
Postnatal day (d)
C
Interval time between mating and delivery(d)
Blank
Saline
Viral injected
D
Dead
Total
Number of newborn offsprings
Blank
Saline
Viral injected

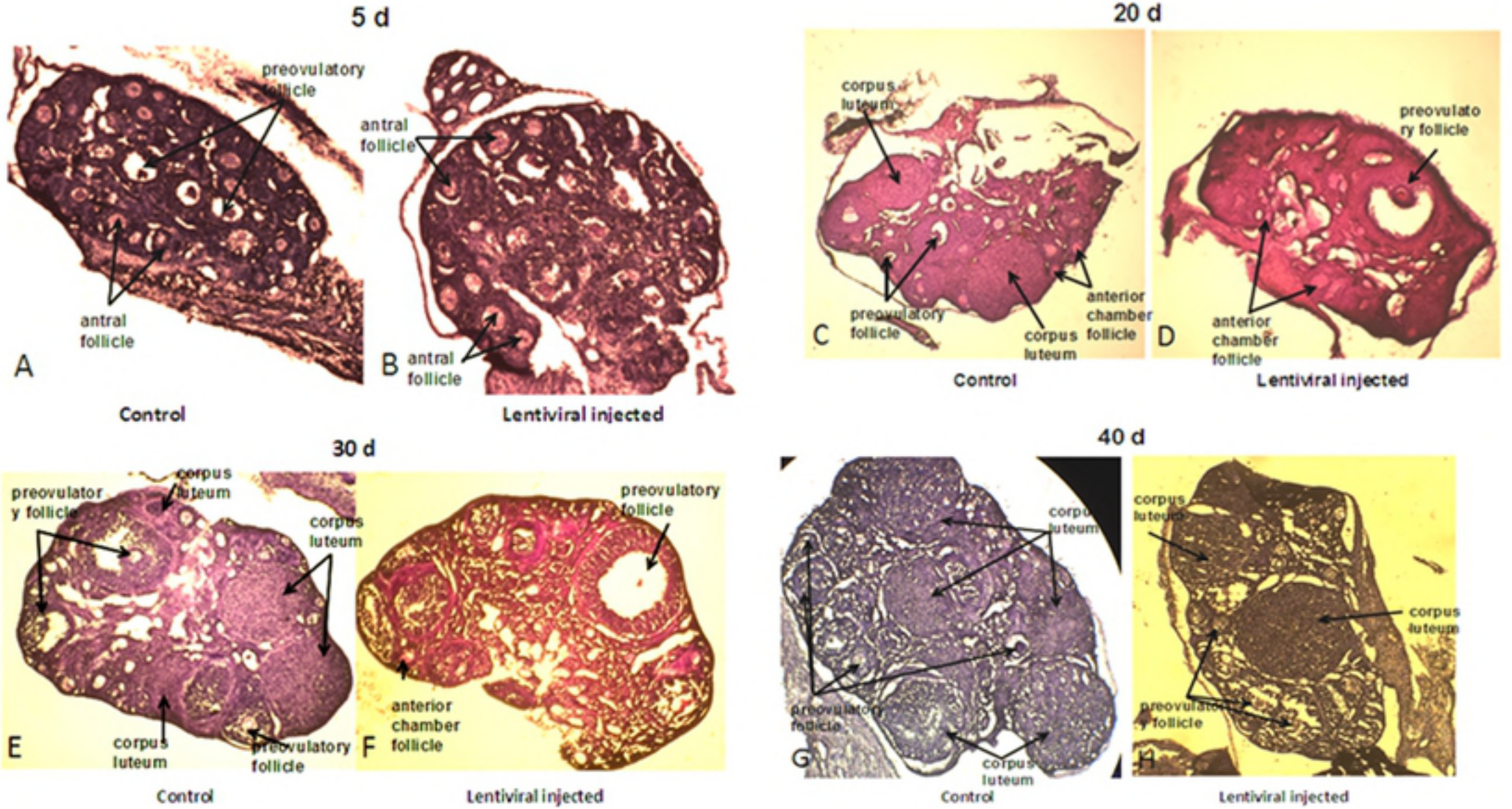
5 d
preovulatory follicle
antral follicle
antral follicle
A
antral follicle
B
Control
Lentiviral injected
20 d
corpus luteum
preovulatory follicle
corpus luteum
anterior chamber follicle
C
preovulato ry follicle
anterior chamber follicle
D
Control
Lentiviral injected
30 d
preovulator y follicle
corpus luteum
corpus luteum
E
corpus luteum
preovulatory follicle
preovulatory follicle
anterior chamber follicle
F
Control
Lentiviral injected
40 d
corpus luteum
preovulatory follicle
G
corpus luteum
Control
corpus luteum
corpus luteum
preovulato ry follicle
H
Lentiviral injected

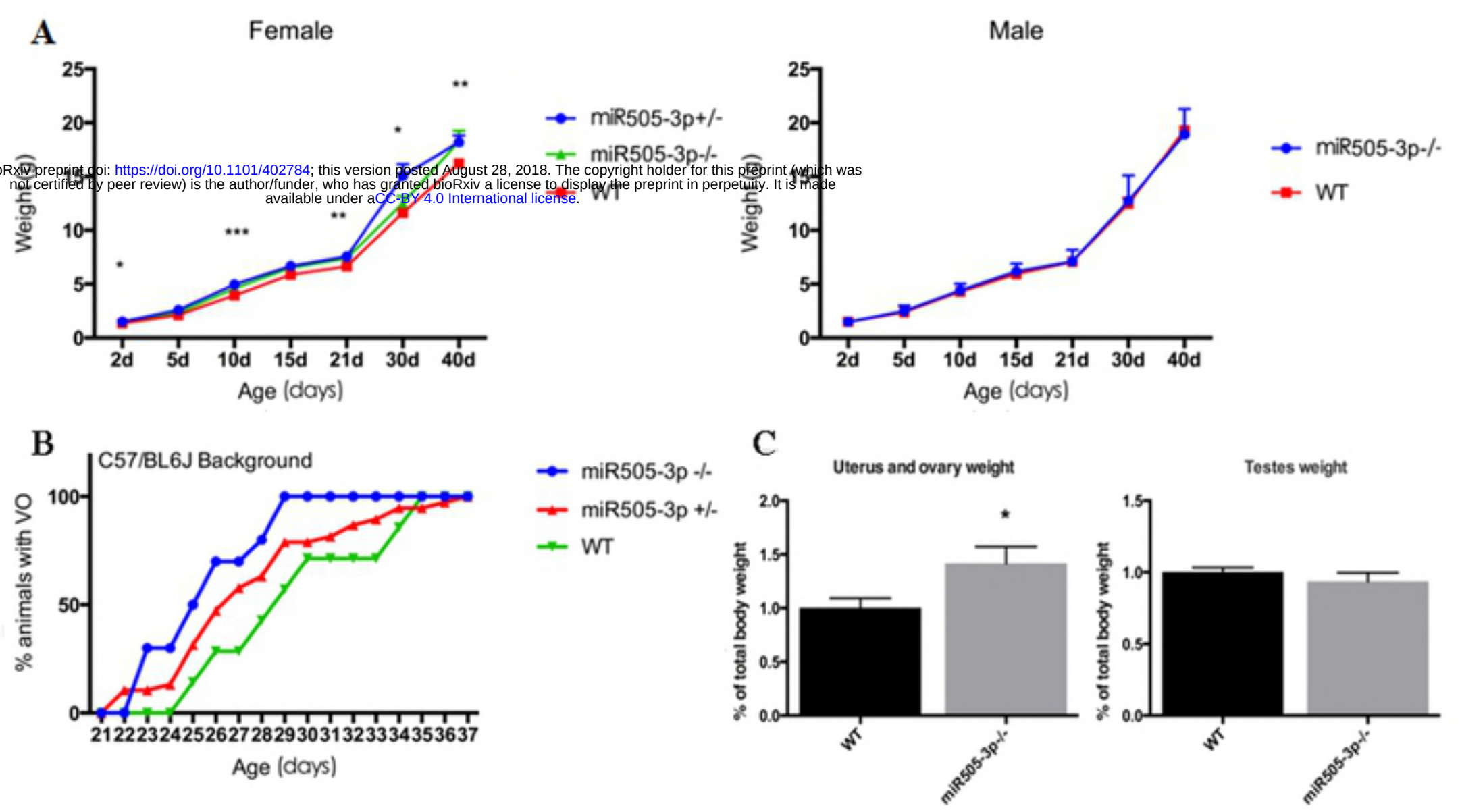

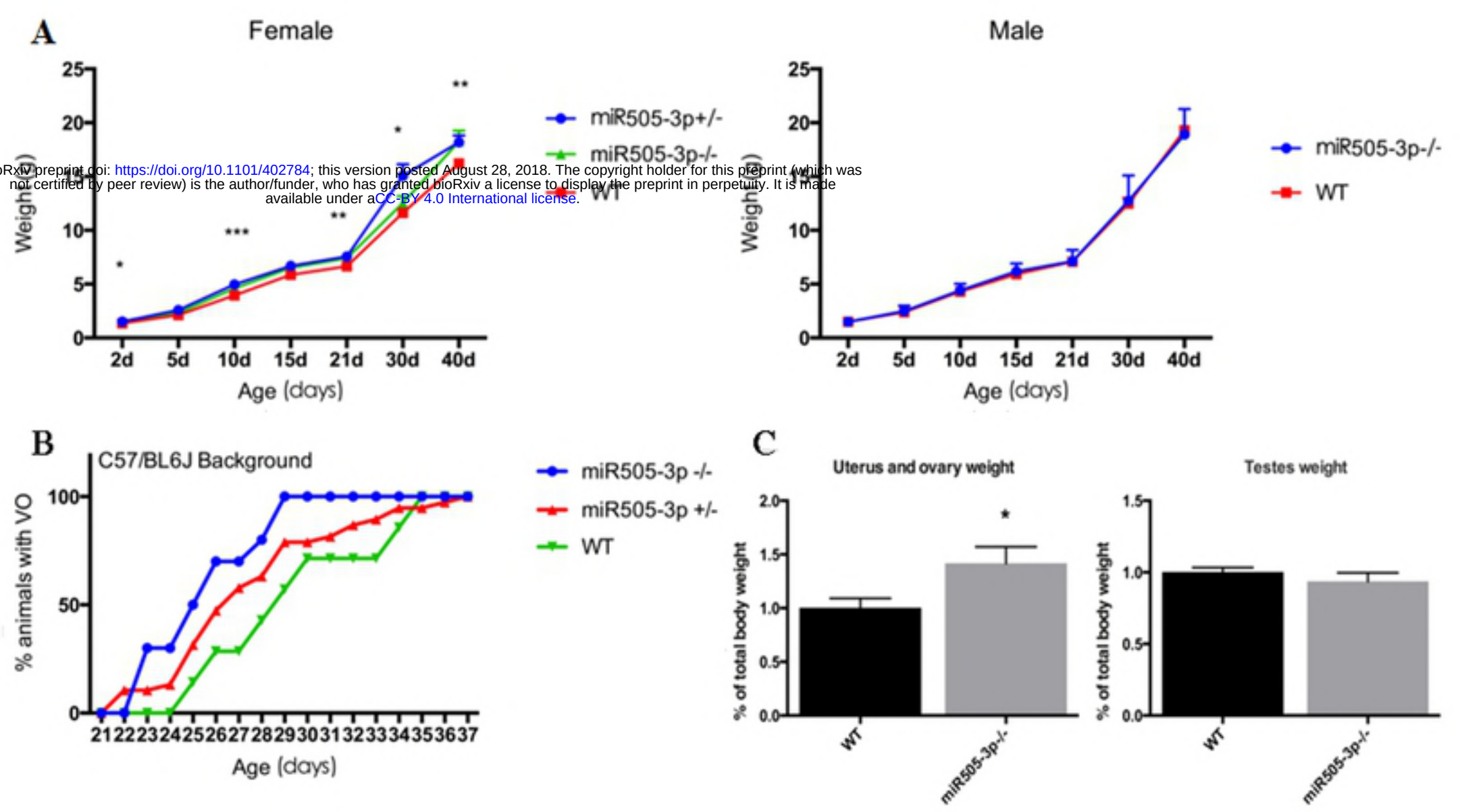

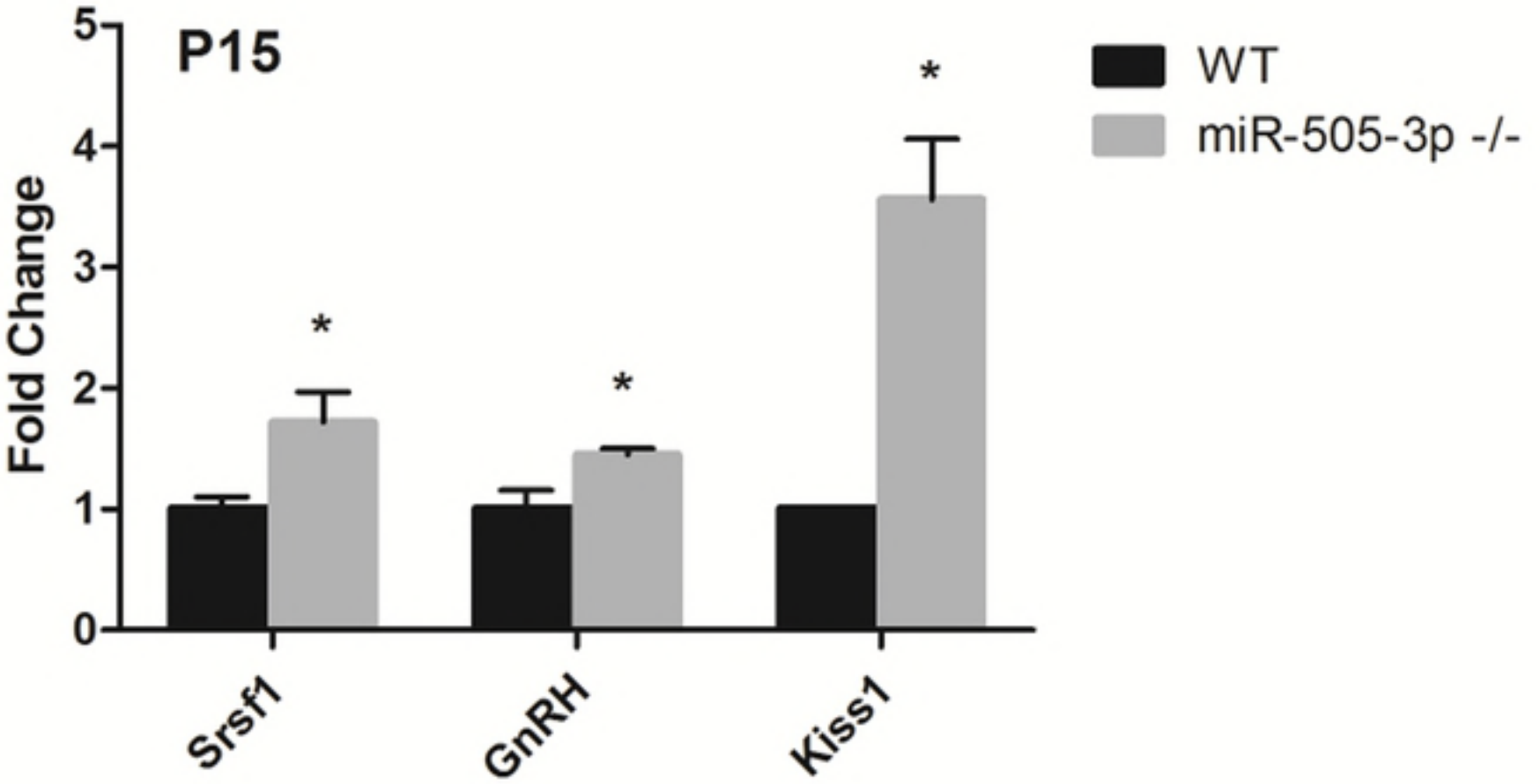

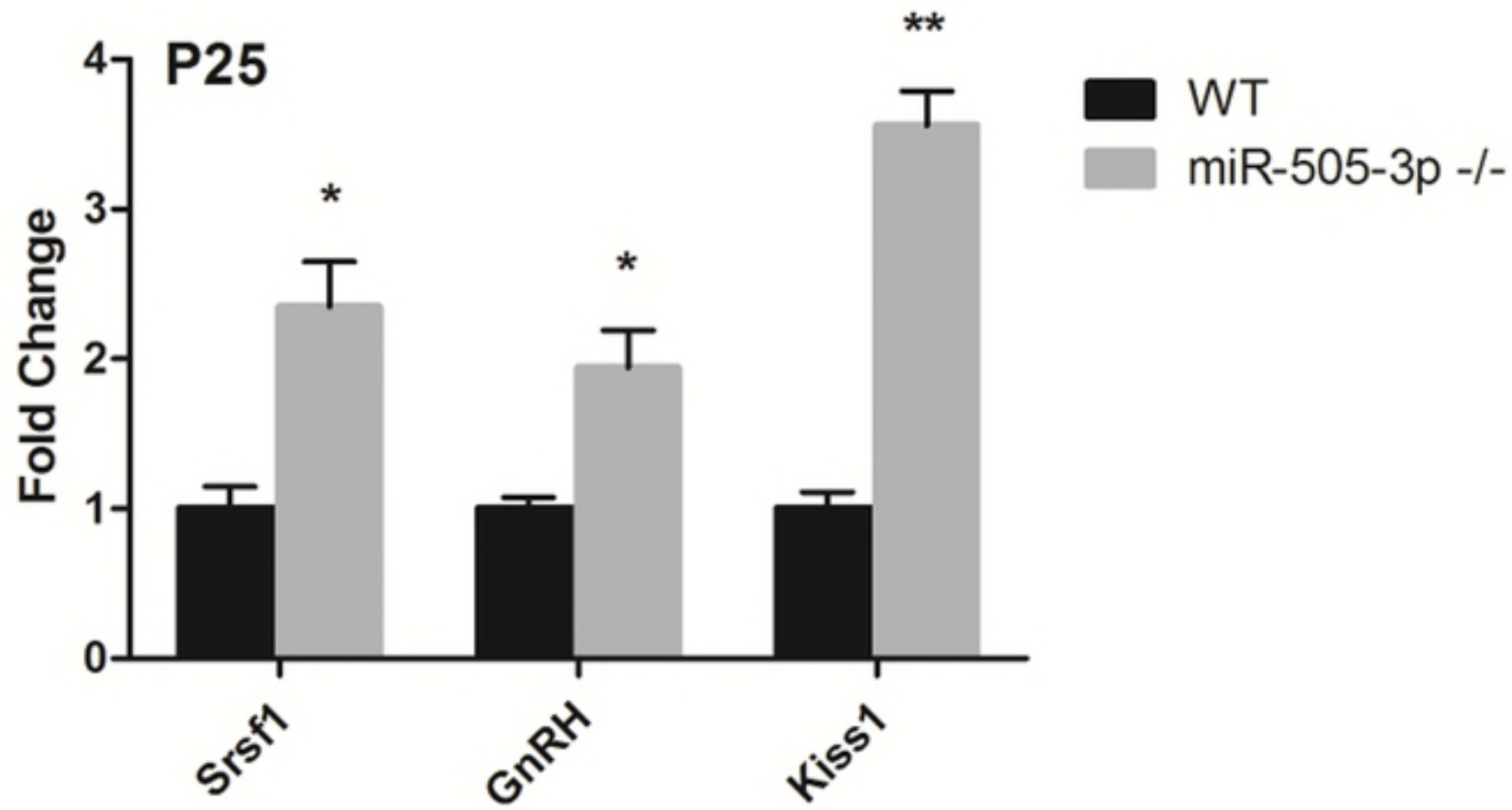

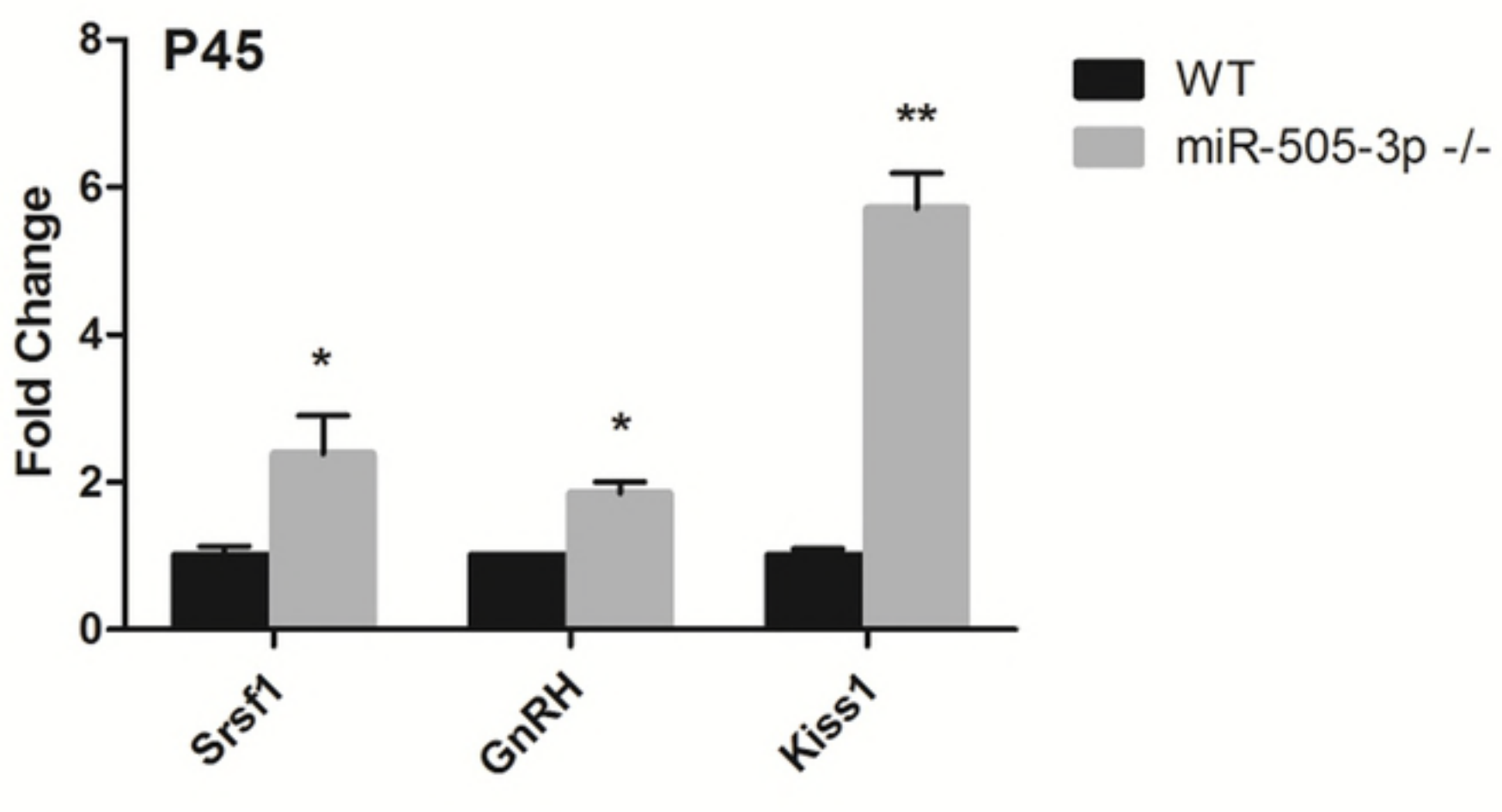

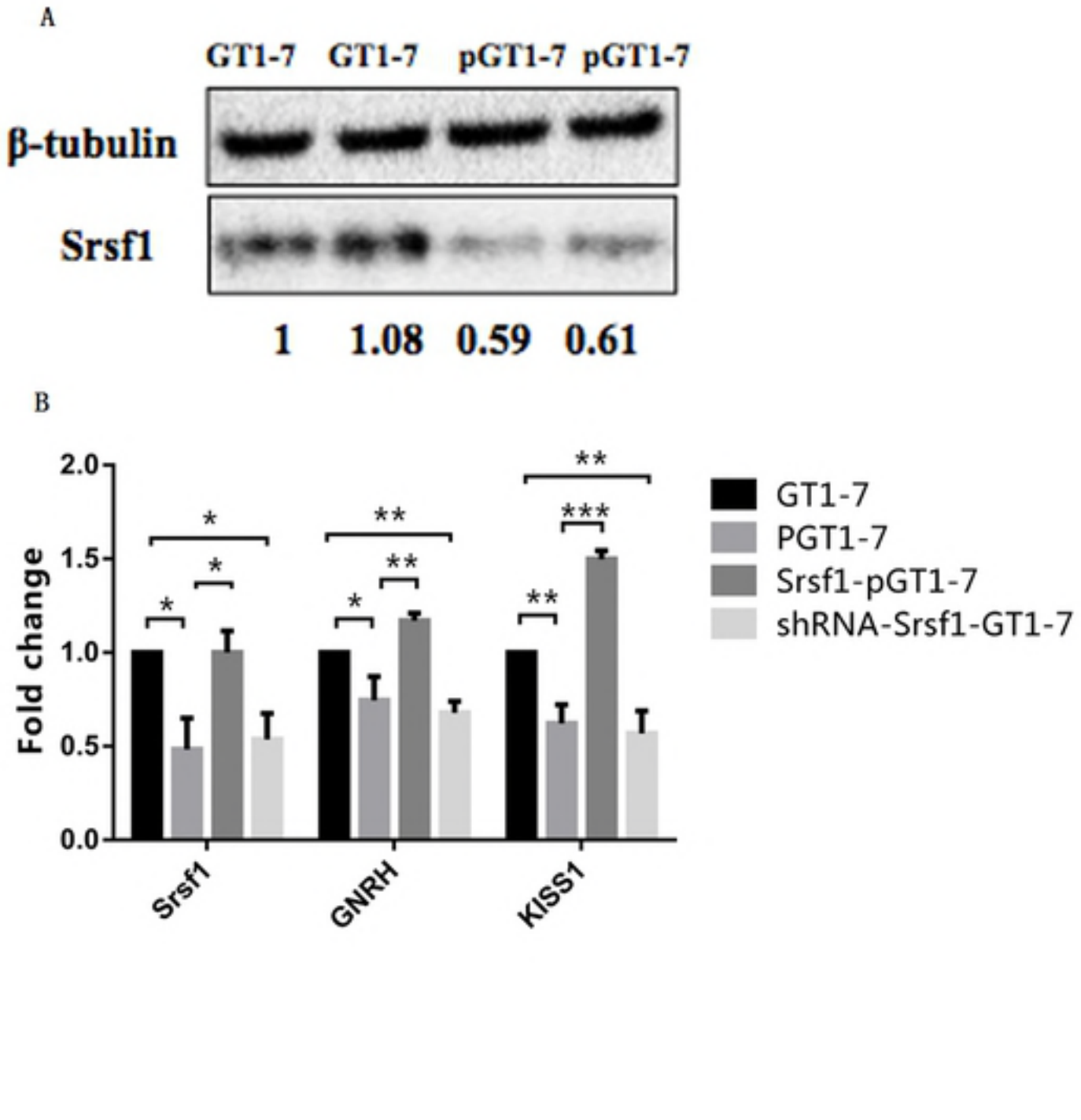
A
GT1-7
GT1-7
pGT1-7
pGT1-7
β-tubulin
Srsf1
1
1.08
0.59
0.61
B
Fold change
2.0
1.5
1.0
0.5
0.0
Srsf1
GNRH
KISS1
GT1-7
PGT1-7
Srsf1-pGT1-7
shRNA-Srsf1-GT1-7
C
P15
P25
P45
Fold Change
Srsf1
GnRH
Kiss1
WT
miR-505-3p -/-

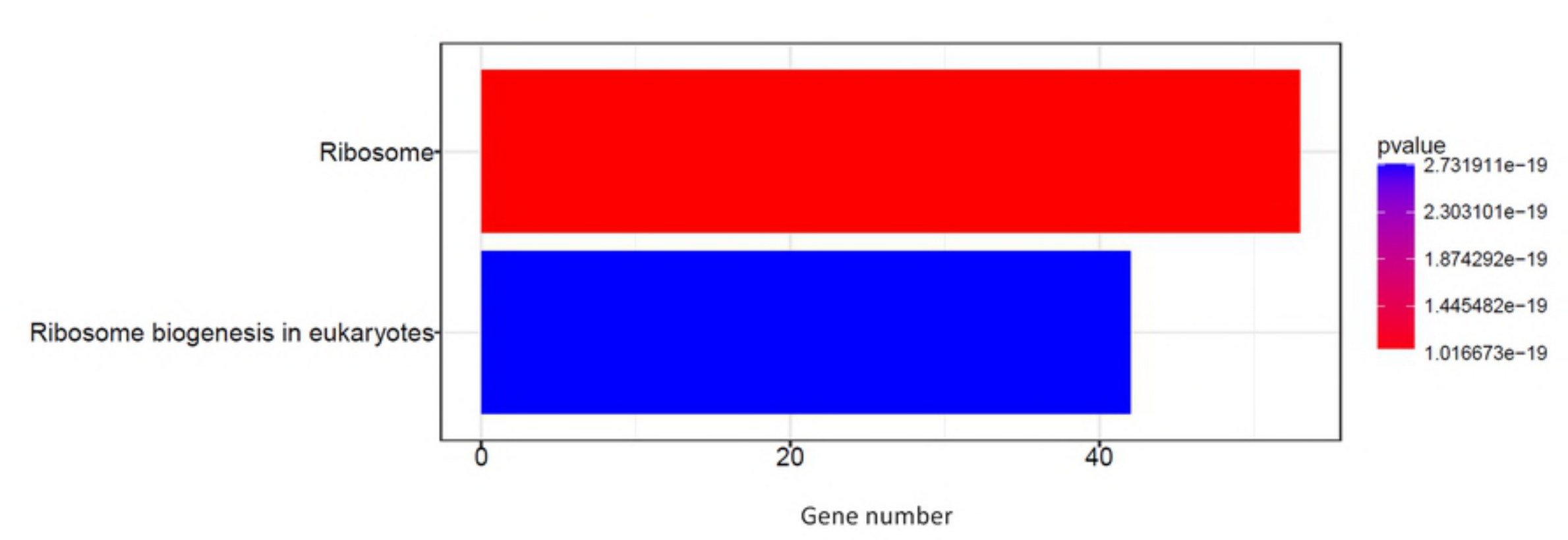
Ribosome
Ribosome biogenesis in eukaryotes
0
20
40
Gene number
pvalue
2.731911e−19
2.303101e−19
1.874292e−19
1.445482e−19
1.016673e−19